Materials Today: Proceedings xxx (xxxx) xxx

Contents lists available at ScienceDirect

Materials Today: Proceedings

journal homepage: www.elsevier.com/locate/matpr

Molecular characteristics of 1-benzhydrylazetidin-3-ol by time-dependent density functional theory analysis

L. Ravindranath [a,*], P. Venkata Ramana Rao [b], K. Srishailam [b], B. Venkatram Reddy [c]

[a] Department of Physics, Malla Reddy Engineering College (A), Hyderabad-500100, Telangana, India
[b] Department of Physics, School of Sciences, SR University, Warangal-506371, Telangana, India
[c] Department of Physics, Kakatiya University, Warangal -506009, Telangana, India

ARTICLE INFO

Article history:
Available online xxxx

Keywords:
UV–Visible spectrum
FMO
NLO
NBO
DFT

ABSTRACT

1-benzhydrylazetidin-3-ol (BA3) molecule was characterized by its experimental UV–Visible (200–400 nm) spectrum in a solution of chloroform and simulated spectrum using time-dependent density functional theory (TD-DFT). The computations were made using density functional theory employing B3LYP exchange–correlation functional in conjunction with the 6–311++G(d,p) basis set. Good agreement was observed between measured and computed quantities corresponding to structure parameters and UV–Visible spectrum. The chemical reactivity of the molecule was identified with the help of frontier molecular orbital (FMO) parameters. The non-linear optical (NLO) behavior of the molecule was studied by computing the values of hyperpolarizability (β_t), polarizability (α_t), and dipole moment (μ_t). NBO analysis has been used to examine the molecule's stability as a result of hyper-conjugative interactions and charge delocalization. According to NBO analysis, the title molecule has O-H• • • N and C-H• • •N bifurcated hydrogen bonds, which is compatible with the result of the molecular structure study. It is evident from the computed HOMO and LUMO energies that charge transfer takes place within the molecule. The NLO parameters also confirm these findings. Thermodynamic parameters were also computed for this molecule.

Selection and peer-review under responsibility of the scientific committee of the 2nd International Conference on Multifunctional Materials.

1. Introduction

The pharmacological and biological effects of medications made of azetidine ring system and their derivatives have been carefully studied [1,2]. Modern aspects of azetidine synthesis were reported by Kurteva [3]. Drugs made out of azetidines are a fascinating class of four-membered nitrogen-containing heterocycles that have recently drawn a lot of interest from chemical researchers [4]. The biological and pharmacological effects of azetidine moiety derivatives have been studied [5,6]. The most crucial component in therapeutic use among the numerous substituted derivatives of azetidine is 3-substituted azetidine [7,8]. The synthesis of the titled compound, 1-benzydrylazetidin-3-ol (BA3), was reported by Krishna Reddy et al [9]. BA3 is widely used in the pharmaceutical intermediate to the synthesis of antiepileptic drugs like Dezinamide [10,11], antihypertensive drugs such as Azetnidipine [12], an oncolytic drug (D83-7676) [13], Oral carbapenem antibiotics that is tebipenem (LJC-11,036) [14], antimicrobial agents(i.e, azetidinyloxy) [15], tebipenem pivixial (L-084) [16] and many more derivatives. Michal Gajhede and co-workers reported the crystal structure and conformation of 3-azetidinol by using the x-ray diffraction method [17]. The hydroxyl moiety occupies various positions concerning the ring and intra-molecular hydrogen bonding between OH and nitrogen atoms along the axial line of the conformer, which is also possible in the case of the condensed phase [17]. This hydrogen bonding and various conformational properties of azetidines attract several researchers. Kolbjorn Hagen et al [18] reported the results of molecular structure and conformational studies of 3-azetidinol using *ab initio* calculations. Anthoni et al [19] used IR, Raman, and ^{1}H NMR spectroscopy and theoretical studies for demonstrating the intra-, and inter-molecular hydrogen bonding, and isomerism of 3-azetidinol.

The composition or length of conjugated -systems may be changed, and the effects of different electron-donor and acceptor groups can be studied to artificially alter nonlinearity in organic

* Corresponding author.
E-mail address: ravi.lyathakula@gmail.com (L. Ravindranath).

https://doi.org/10.1016/j.matpr.2023.05.003
2214-7853/
Selection and peer-review under responsibility of the scientific committee of the 2nd International Conference on Multifunctional Materials.

chromophores. Nevertheless, since the computed ring atom charge densities are very dependent on the calibre of the basis sets used, it is impossible to predict with any degree of accuracy whether an aromatic ring would be electron-rich or electron poor. Since the NLO properties depend on the degree of intramolecular charge transfer (ICT) interaction across the conjugative paths and the ability of an aromatic ring to transfer electrons is largely influenced by its ionization potential (IP) and electron affinity (EA), which, according to molecular orbital theory and Koopman's theorem [20], are equal to the negative of HOMO and LUMO energies, respectively, a reliable trend of the electron releasing/withdrawing strengths of the heterocycles may be predicted on the basis of the computed frontier orbital energies [21,22]. Our most recent publications on such biologically active compounds [23–25].

Hence, we considered it important to conduct an experimental and theoretical analysis of BA3. As a result, we suggest that,

1) Record the UV–Visible spectrum of BA3
2) Carry out DFT calculations on the titled molecule in order to:
(i) optimize the equilibrium geometry.
(ii) study electronic properties comprising of UV–Visible spectrum, HOMO and LUMO energies, and electrostatic potential surface (MESP).
(iii) examine non-linear optical(NLO) behavior, natural bond orbital (NBO) characteristics, and thermodynamic parameters in order to enhance the comprehensive nature of these investigations.

2. Measurement of spectra

The titled molecule was purchased from Aldrich chemical company, USA. This compound 1-benzhydrylazetidin-3-ol is a solid at room temperature. The UV–Visible spectrum of the BA3 was recorded with a Perkin-Elmer UV–Vis LAMBDA-25 double-beam spectrometer in a solution of DMSO d_6 in the spectral range of 200–400 nm.

3. Computational considerations

To compute required molecular characteristics connected to electronic transitions, Frontier molecular orbital behavior, NLO parameters, NBO behavior, and MESP of BA3, we utilized density functional theory (DFT) which was incorporated in the gaussian 09 W software package [26]. These calculations were performed with three components proposed by Beck B3 [27] along with Lee-Yang-Parr [28] correlational functional and in combination with 6–311++G(d,p) split valence triple zeta basis set.

TD-DFT (time-dependent density functional theory) was used to simulate the UV–Visible absorption spectrum of BA3 in a solution of DMSO d_6 (used solvent to measure the experimental spectrum) [29–31].

The significant parameters like Chemical potential (μ), global electrophilicity index (ω), global chemical softness (ζ), electron affinity(A), electronegativity (χ), and ionization potential (I) of BA3 were evaluated using the computed values of HOMO (highest occupied molecular orbital) and LUMO (lowest unoccupied molecular orbital) energies employing DFT [32–35].

In the usual process, the nonlinear optical properties of the given molecule are analyzed in terms of its total molecular polarisability (α_t), anisotropy of polarizability ($\Delta\alpha$), and static hyperpolarizability (β_t) of the first order, and total molecular dipole moment (μ_t). These parameters were calculated with DFT in combination with Buckingham Formalism [36] based on the finite field method [37].

The arrangement of the -electrons between the two phenyl rings is a noteworthy structural characteristic of BA3. This is required to quantify the aspect of the molecule described in the title. This contributes to the comprehension of the various second-order interactions linking the occupied orbitals of one subsystem and the vacant orbitals of another subsystem. By subjecting their Fock matrices to NBO-based second-order investigations, BA3 molecules' donor–acceptor interactions are evaluated for this purpose. These interactions manifest as a transfer of occupancy from the localized non-Lewis orbital (NBO) of the idealized Lewis structure to an empty non-Lewis orbital. Thus, we made use of NBO version 3.1 [38], which is a component of the Gaussian 09 W programme.

4. Results and discussion

4.1. Molecular geometry in the ground state

Molecular geometry optimized by solving iteratively, self-consistent field equations for BA3 as shown in Fig. 1, along with the numbering of atoms. The structural data containing bond lengths, bond angles, and dihedral angles for the titled molecule are presented in Table 1. The computed geometrical parameters of BA3, compared with experimental counterparts of related molecules [17,39]. It is observed that the molecule BA3 attained a non-planar configuration of C_1 symmetry from the DFT calculations.

4.2. Frontier molecular orbitals

Frontier molecular orbitals (FMOs) (i.e, HOMO and LUMO) simplify proper understanding of the electronic transitions and chemical activity. FMOs play a vital role in quantum chemistry for the identification and prediction of the chemical reactivity of conjugated systems [40]. HOMO and LUMO energies provide an electron donor and an electron acceptor [32], respectively.

4.2.1. Analysis of UV–Vis spectrum

The UV–Visible absorption spectrum of BA3 was computed with the help of calculations using the TD-DFT/B3LYP/6-311++G(d,p) method using the Polarisable Continuum Model (PCM) [41,42]. The observed and simulated UV–Vis spectrum of the molecule BA3 was depicted in Fig. 2, and corresponding signal values were reported in Table 2.

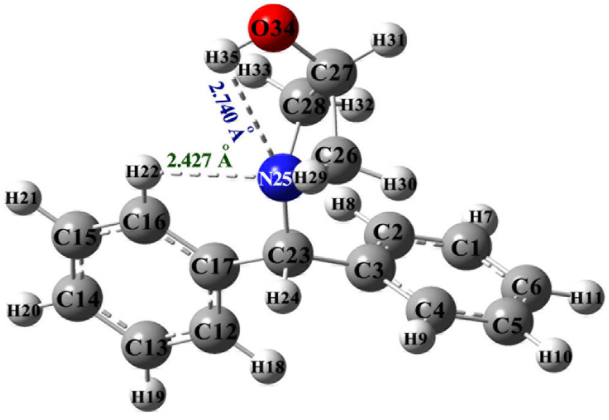

(E_{BA3} = - 1969.293 x 10^3 kJ mol^{-1})

Fig. 1. Optimized molecular structure of BA3 monomers along with numbering of atoms and minimum energy.

Table 1
Experimental and DFT/B3LYP/6-311 ++ G(d,p) optimized geometric parameters of BA3.

Geometric parameter	Calculated Value	Expt. Value[a]	Geometric parameter	Calculated Value	Expt. Value[a]	Geometric parameter	Calculated Value	Expt. Value[a]
Bond lengths (in Å)			**Bond angle (in °)**					
C1-C2	1.393	1.390	C1-C2-C3	120.87	119.9	N25-C26-C27	88.25	90.4
C2-C3	1.401	1.383	C2-C3-C4	118.20	119.3	C26-C27-C28	85.99	89.7
C3-C4	1.399	1.372	C3-C4-C5	121.13	120.3	C27-C28-N25	88.08	89.1
C4-C5	1.395	1.380	C4-C5-C6	120.01	120.7	C26-N25-C28	90.98	89.3
C5-C6	1.393	1.360	C5-C6-C1	119.52	119.7	C26-C27-O34	115.49	115.1
C6-C1	1.395	1.380	C6-C1-C2	120.27	119.9	C28-C27-O34	115.61	113.5
C12-C13	1.392	1.415	C12-C13-C14	120.23	119.5	**RMSD**	**2.142**	
C13-C14	1.395	1.343	C13-C14-C15	119.31	123.4	**Dihedral angle (in °)**		
C15-C16	1.395	1.371	C15-C16-C17	120.83	125.3	C26-N25-C28-C27	19.8	18.08[b]
C16-C17	1.397	1.375	C16-C17-C12	118.31	121.1	C23-N25-C28-C27	146.6	–
C17-C12	1.401	1.388	C13-C12-C17	120.95	118.7	C28-N25-C26-C27	19.8	18.08[b]
C3-C23	1.530	1.517	C2-C3-C23	121.79	123.1	C23-N25-C26-C27	−151.2	–
C17-C23	1.532	1.535	C4-C3-C23	119.95	117.6	N25-C28-C27-C26	−18.9	−17.60[b]
C23-N25	1.469	1.468	C12-C17-C23	120.14	–	N25-C28-C27-O34	−97.4	–
N25-C26	1.479	1.525	C16-C17-C23	121.45	123.1	N25-C26-C27-C28	19.0	17.60[b]
C26-C27	1.549	1.535	C3-C23-C17	113.70	114.8	N25-C26-C27-O34	97.5	–
C27-C28	1.549	1.537	C3-C23-N25	113.51	109.6	**RMSD**	**1.546**	
N25-C28	1.484	1.559	C17-C23-N25	111.69	110.5	**Intra-molecular H-bond length (in Å)**		
C27-O34	1.415	1.413	C23-N25-C26	120.64	119.3	H22·····N25	2.427	–
RMSD	**0.028**					H35·····N25	2.740	–

[a] : From Ref. [39]; b: From Ref. [17]; -: Not available.

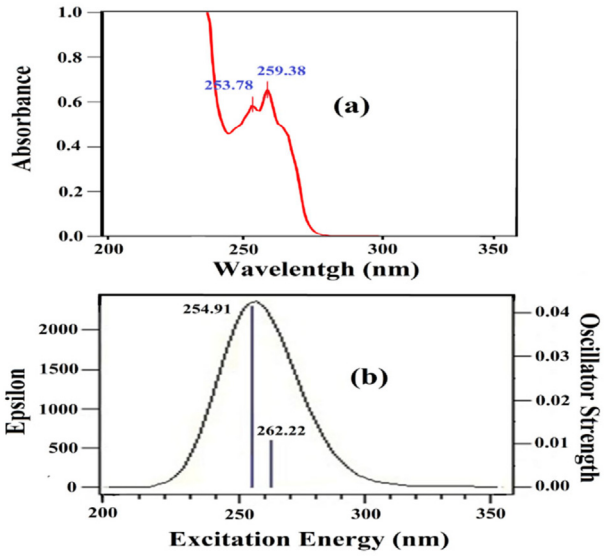

Fig. 2. UV–Vis Spectrum of BA3 (a) Experimental and (b) Simulated with DFT/B3LYP/6-311++G(d,p) formalism.

4.2.2. Chemical reactivity descriptors

Chemical reactions are significantly influenced by FMOs and their attributes, such as energy. To demonstrate a molecule's chemical reactivity, polarizability, and kinetic stability, one can use the frontier orbital energy gap between HOMO and LUMO [43]. Because it takes more energy to excite electrons from a HOMO to a LUMO, a small HOMO-LUMO energy gap suggests low kinetic stability and strong chemical reactivity [44], whereas a large HOMO–LUMO energy gap indicates a harder molecule. Soft molecules are known to be more polarizable and, as a result, more reactive chemically than hard molecules [45]. This is due to the fact that they have a smaller energy gap. A measure of how many electrons are transferred between a donor and an acceptor is called electrophilicity [46].

The HOMO-LUMO orbital energies and various investigated parameters obtained from the computations using DFT/B3LYP/6-311++G(d,p) level of theory for BA3 are presented in Table 3 (see Fig. 3 also).

4.3. Non-linear optical (NLO) characteristics

NLO materials have interacted with electromagnetic radiation resulting in a change of significant propagation characteristics of the incident radiation i.e, frequency, phase, and amplitude producing new fields [47]. These changes are important for the non-linear optical material used for switching, frequency shifting, and optical logic. These effects of NLO materials are declared by the value of their first-order hyperpolarizability.

The NLO performance of a molecular system is generally evaluated by comparing its total molecular dipole moment (μ_t) and the mean first-order hyperpolarizability (β_t) with the corresponding quantities of anarchetypicalmolecule like Urea. μ_t and β_t for Urea is 1.3732 Debye and 372.8 $\times$ 10^{-33} cm^5/esu, respectively, which are used frequently as threshold values. μ_t is computed at 0.7587 Debye and β_t for them is predicted near 412.6970 $\times$ 10^{-33} cm^5/

Table 2
Experimental and theoretical (DFT/B3LYP/6-311++G(d,p) formalism) electronic absorption spectral values for BA3.

Absorption Maximum λ_{max}(nm)		Excitation Energies (eV)	Oscillator Strengths (f)	Major contribution (≥10%)	Transition
Expt.	**Cal.**				
259.38	262.22	4.7283	0.0107	H → L (97%)	π → π*
253.78	254.91	4.8637	0.0414	H → L + 1 (95%)	π → π*

H: HOMO; L: LUMO.

Table 3
Frontier molecular orbital parameters of BA3.

Frontier molecular orbital parameter	Value (in eV)
HOMO energy	−8.9019
LUMO energy	−5.3095
Frontier molecular orbital energy gap	3.5924
Ionization energy (I)	8.9019
Electron affinity (A)	5.3095
Global chemical hardness (η)	1.7962
Global chemical softness (ζ)	0.2784
Chemical potential (μ)	−7.1057
Electronegativity (χ)	7.1057
Global electrophilicity power (ω)	14.0567

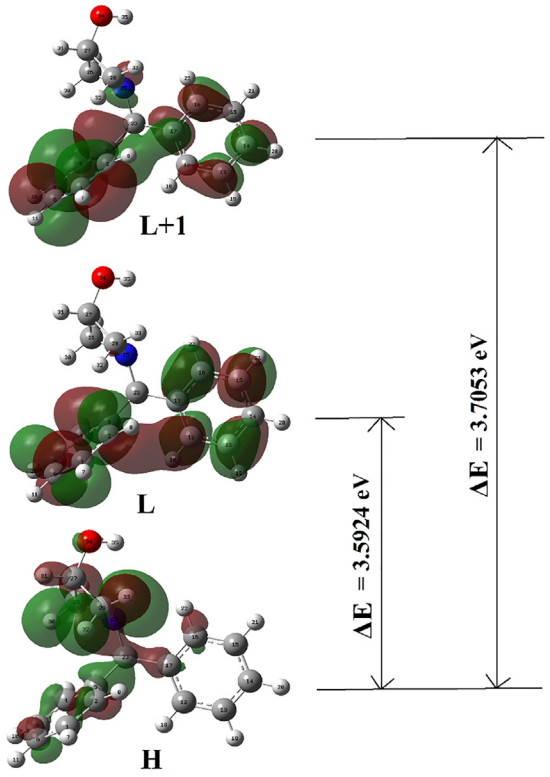

Fig. 3. Frontier molecular orbitals of BA3.

esu. Thus, we find that the value of μ_t lower than the threshold value of Urea, while the value of β_t is 1.12 times higher than the threshold value of Urea. Hence, due to this relatively higher value of hyperpolarizability, with respect corresponding parameter for Urea, the titled compound is a potential candidate for NLO applications. The greatest charge delocalization takes place along β_{yyy} in the molecule BA3, as substantiated by Table 4.

Table 4
Values of dipole moment, μ_t (in Debye); polarizability, α_t in 1.4818 × 10^{-25} cm^3; and first order hyperpolarizability, β_t (in 8.641 × $10^{-33}$$cm^5$/e.s.u) of BA3 by DFT/ B3LYP/6–311++G(d,p) method.

Type of component	Value	Type of component	Value
μ_x	−0.0924	β_{xxx}	−8.8415
μ_y	−0.7443	β_{xxy}	−47.5922
μ_z	−0.1150	β_{xyy}	−61.3860
μ_t	**0.7587**	β_{yyy}	−352.7448
α_{xx}	223.2837	β_{xxz}	14.0454
α_{xy}	16.4138	β_{xyz}	6.4523
α_{yy}	203.5325	β_{yyz}	−8.7627
α_{xz}	12.3438	β_{xzz}	5.5122
α_{yz}	−2.8472	β_{yzz}	−6.5951
α_{zz}	154.2493	β_{zzz}	−28.5296
α_t	**193.6885**	**β_t**	**412.6970**
$\Delta\alpha$	**61.5820**		

4.4. Thermodynamic parameters and rotational constants

Table 5 shows several rotational constants and derived thermodynamic parameters for BA3. Standard expressions are used in the rigid rotor harmonic oscillator approximation to compute the standard thermodynamic functions, including SCF energy, specific heat capacity at constant volume (Cv), entropy (S), vibrational energy (Evib), zero-point energy (E0), and rotational constants (A, B, and C) [48,49], using DFT/B3LYP/6-311++G(d,p) level of theory. The rotational constants A, B, and C are calculated at 451.60, 386.16, and 234.63 MHz, respectively, for BA3. These thermodynamic parameters were computed in the gas phase and concerned with one mole of perfect gas at one-atmosphere pressure.

4.5. Natural bond orbital (NBO) analysis

The NBO analysis describes the hyper conjugative interactions of the Fock matrix with the second-order perturbation theory using the NBO 3.1 program [38] as implemented in the Gaussian 09 W software at the DFT/B3LYP level using 6–311++G(d,p) basis set. It includes the maximum possible percentage of electron density (ED) which helps in a clear understanding of intra-molecular charge transfer (ICT), intra- and inter-molecular bonding interactions, and hyper-conjugative interactions between the donor (i) and acceptor (j) groups within a given electronic structure.

Let us consider the stabilization energy E(2), associated with donor (i) to an acceptor (j) electron delocalization, as estimated using the equation [49,50].

$$E(2) = -q_i \frac{F_{ij}^{22}}{\Delta E} = -q_i \frac{\langle i|F|j\rangle^2}{\varepsilon_j - \varepsilon_i}$$

where q_i is the donor orbital occupancy, ε_i and ε_j are energies of i^{th} and j^{th} orbitals (diagonal elements), respectively, and F_{ij} is the off-diagonal NBO Fock matrix element.

The largest value of stabilization energy E(2) indicates a strong interaction between the electron donors and electron acceptors resulting in a greater extent of conjugation of the whole system. The dominant contributors to the stabilization energies, that emerge from NBO analysis for BA3 are presented in Table 6. The delocalization of ED, between occupied Lewis-type (bonding or lone pair) NBO orbitals and empty non-Lewis (anti-bonding or Rydberg) NBO orbitals implies stabilization of donor–acceptor interaction. Intra-molecular hyper conjugative interactions arise due to overlap between the bonding π-orbitals and anti-bonding π*-orbitals. For BA3, the values of ED at the conjugated π-bonds

Table 5
Thermodynamic parameters (for one mole of perfect gas at one atm) and rotational constants of BA3.

Thermodynamic parameters	Value
SCF Energy (in 10^3 kJ mol^{-1})	−1969.293
Total energy (thermal), E_{total} (kcal mol^{-1})	193.518
Heat capacity at const. volume, C_V (cal $mol^{-1}K^{-1}$)	60.624
Heat capacity at const. pressure, C_P (cal $mol^{-1}K^{-1}$)	62.610
Entropy, S (cal $mol^{-1}K^{-1}$)	125.881
Vibrational energy, E_{vib} (kcal mol^{-1})	191.741
Zero-point vibrational energy, E_0 (kcal mol^{-1})	183.967
Rotational constants (MHz)	
A	451.60
B	386.16
C	234.63

Table 6
Second-order perturbation theory analysis of FOCK matrix in NBO basis corresponding to the intra-molecular bonds of BA3 by DFT/B3LYP/6-311++G(d,p) method.

NBO(i)	Type	ED/e	NBO(j)	Type	ED/e	E(2)[a] (kcal/mol)	E(j)-E(i)[b] (a.u)	F(i,j)[c] (a.u)
C1-C2	π	1.66622	C3-C4	π*	0.34840	20.77	0.29	0.069
			C5-C6	π*	0.32902	20.16	0.28	0.067
C3-C4	π	1.65883	C1-C2	π*	0.32137	19.75	0.28	0.067
			C5-C6	π*	0.32902	20.62	0.28	0.068
C5-C6	π	1.66743	C1-C2	π*	0.32137	20.16	0.28	0.068
			C3-C4	π*	0.34840	19.86	0.29	0.068
C12-C13	π	1.67211	C14-C15	π*	0.33096	20.01	0.28	0.067
			C16-C17	π*	0.34089	20.43	0.29	0.069
C14-C15	π	1.67033	C12-C13	π*	0.32427	20.39	0.28	0.068
			C16-C17	π*	0.34089	19.77	0.29	0.068
C16-C17	π	1.65517	C12-C13	π*	0.32427	20.02	0.28	0.067
			C14-C15	π*	0.33096	20.78	0.28	0.068
LP(1)N25		1.87624	C3-C23	σ*	0.04113	7.40	0.69	0.065
			C26-H30	σ*	0.02677	6.41	0.68	0.060
			C28-H32	σ*	0.02592	6.12	0.69	0.059
LP(2)O34		1.95045	C26-C27	σ*	0.02605	6.37	0.64	0.057
			C27-C28	σ*	0.02612	6.76	0.64	0.059

[a] : E(2) means the energy of hyper conjugative interaction (stabilization energy).
[b] : Energy difference between the donor (i) and an acceptor (j) NBO orbitals.
[c] : F(i,j) is the Fock matrix element between i and j NBO orbitals.

are between 1.65517 and 1.67211, as can be seen from Table 6, whereas the corresponding values, for π*-anti-bonds are in the range 0.32137–0.34840. According to NBO analysis, the interactions π(C1-C2) → π*(C3-C4 and C5-C6); π(C3-C4) → π*(C1-C2 and C5-C6); π(C5-C6) → π*(C1-C2 and C3-C4); π(C12-C13) → π*(C14-C15 and C16-C17); π(C14-C15) → π*(C12-C13 and C16-C17); and π(C16-C17) → π*(C12-C13 and C14-C15) possesses high stabilization energy in the range 19.75–20.78 kcal mol^{-1}, respectively. Based on this observation, it can be stated that the NLO properties of BA3 originate from ICT. This statement substantiates the conclusion arrived at in section 4.3, Non-linear optical (NLO) properties.

4.6. Analysis of molecular electrostatic surface potential (MESP)

By identifying electrophilic and nucleophilic areas in a molecule, the molecular electrostatic surface potential (MESP) is a well-known method for understanding molecular reactivity features. MESP is connected to a specific molecule's dipole moment, partial charges, chemical reactivity, and electronegativity [50], non-covalent interactions, in particular hydrogen bonds [51], molecular aggregation [52], lone pair interactions [53], aromaticity, and reaction mechanisms [54]. MESP has been developed using the DFT/B3LYP/6-311++G(d,p) formalism for the BA3 molecule. In the MESP diagram, the negative (electron-rich) regions are coloured red and are associated with electrophilic reactivity, whereas the positive (electron-deficient) parts are coloured blue and are associated with nucleophilic reactivity. For the chemical under research, the MESP map is displayed in Fig. 4. This Fig. 4 demonstrates that the greatest negative and positive regions.

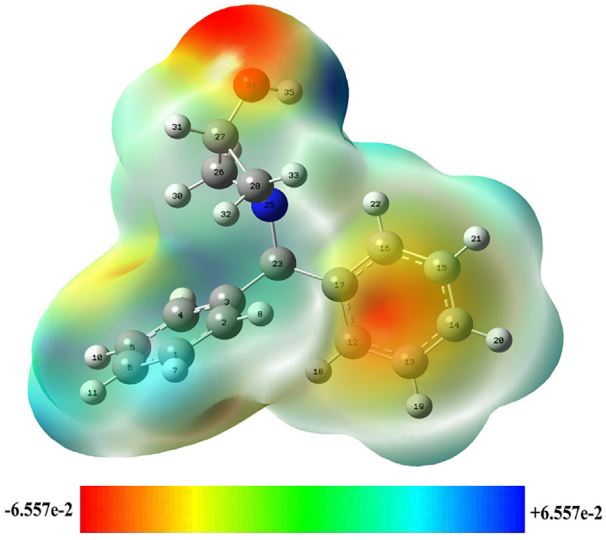

Fig. 4. Total electron density mapped with an electrostatic potential surface of BA3.

5. Conclusions

BA3 molecule is a non-planar with C_1 point group symmetry and forms bifurcated intra-molecular hydrogen bonds between (H22, N25); and (H35, N25) atoms. Computed values of FMO reveal that BA3 is highly reactive as the energy gap was small at 3.5924 eV, and assisted in the assignment of observed UV–Vis spectral bands. The results showed that BA3 made excellent candidates for NLO applications. NBO analysis was used to demonstrate that the NLO characteristics of this molecule were caused by intramolecular charge transfer (ICT). By analysis of the MESP surface, the most reactive sites are located around the nitrogen and oxygen atoms of the azetidine moiety in BA3. The standard thermodynamic functions, such as heat capacity at constant pressure (C_P), heat capacity at constant volume (C_v), and entropy (S), were calculated for BA3. Other parameters, such as rotational constants (A, B, and C), zero point vibrational energy (E_o), and self-consistent field (SCF) energy, were also calculated.

CRediT authorship contribution statement

L. Ravindranath: . **P. Venkata Ramana Rao:** Conceptualization. **K. Srishailam:** Data curation, Methodology. **B. Venkatram Reddy:** Writing – original draft.

Data availability

No data was used for the research described in the article.

Declaration of Competing Interest

The authors declare the following financial interests/personal relationships which may be considered as potential competing interests: L. Ravindranath reports administrative support was provided by Malla Reddy Engineering College. L. Ravindranath reports a relationship with Malla Reddy Engineering College that includes: employment. L. Ravindranath has patent #Investigation of molecular structure, UV-Visible spectral studies, chemical reactivity and other molecular characteristics of 1-benzhydrylazetidin-3-ol by DFT analysis pending to L. Ravindranath. The authors declare that they have no known competing financial interests or personal relationships that could have appeared to influence the work reported in this paper.

Acknowledgments

The authors sincerely acknowledge NIT Warangal for UV-Vis spectral measurements. The first author (LRN) is grateful to the management of Malla Reddy EngineeringCollege (Autonomous), Hyderabad, India, and the second and third authors (PVRR & KSS) thank the management of SR University, Warangal, India, for their support and encouragement during this research work.

References

[1] M. D'hooghe, N. De Kimpe, In: ComprehensiVe Heterocyclic ChemistryIII. Stevens CV. Elsevier:Oxford, U.K: 2008, Vol. 2, Chapter 2.01, p. 1.
[2] N. De Kimpe, in: Comprehensive Heterocyclic Chemistry II. Padwa A.Elsevier: Oxford, U.K:1996, Vol. 1B, Chapter 1.18, p. 507.
[3] V. Kurteva, In Modern Approaches to the Synthesis of O- and N-Heterocycles, Kaufman T, Larghi E. 3 (2007) 45.
[4] A.R. Katritzky, A.F. Pozharskii, Handbook of Heterocyclic Chemistry, 2nd ed., Elsevier Science, Amsterdam, 2000.
[5] F. Couty, G. Evano, D. Prim, Mini-ReV. Org. Chem. 1 (2004) 133–148.
[6] G.B. Evans, R.H. Furneaux, B. Greatrex, A.S. Murkin, V.L. Schramm, P.C. Tyler, J. Med. Chem. 51 (2008) 948–956.
[7] D. Honcharenko, J. Barman, O.P. Varghese, Chattopadhyaya, J. Biochem. 46 (2007) 5635–5646.
[8] J. Slade, J. Bajwa, H. Liu, D. Parker, Chen G.P. Vivelo, J. Calienni, E. Villhauer, K. Prasad, O. Repic, T. Blacklock, J. Org. Process Res. Dev. 11 (2007) 825–835.
[9] V.V.R.M. Krishna Reddy, D. Udaykiran, U.S. Chintamani, E. Mahesh Reddy, C.h. Kameswararao, G. Madhusudhan, Development of an Optimized Process for the Preparation of 1-Benzylazetidin-3-ol: An Industrially Important Intermediate for Substituted Azetidine, J. Org. Process Res. Dev. 15 (2011) 462–466, https://doi.org/10.1021/op100247m.
[10] M. Abou-Gharbia, J.A. Moyer, Drugs Future 16 (1991) 3–201.
[11] D.N. Johnson, M. Osman, L. Cheng, E. Swinyard, Epilepsy Res. 5 (1990) 185–191.
[12] Y. Yagil, M. Miyamoto, L. Frasier, K. Oizumi, H. Koike, Am. J. Hypertens. 7 (1994) 637–646.
[13] H. Naito, S. Ohsuki, A. Ejima, C. Makino, H. Ohki, Pyrazole derivatives and salts there of. PCT Int. Appl. WO/2000/005230, 2000.
[14] T. Isoda, I. Yamamura, S. Tamai, T. Kumagai, Y. Nagao, Chem. Pharm. Bull. 54 (2006) 1408–1411.
[15] M.A.W. Wells, C.M. Boggs, B.D. Foleno, E. Wira, K. Bush, R.M. Goldschmidt, D.J. Hlasta, Bioorg. Med. Chem. Lett. 11 (2001) 1829–1832.
[16] T. Isoda, H. Ushirogochi, K. Satoh, T. Takasaki, I. Yamamura, C. Sato, A. Mihira, T. Abe, S. Tamai, S. Yamamoto, T. Kumagai, Y. Nagao, J. Antibiot. 59 (2006) 241–247.
[17] M. Gajhede, U. Anthoni, C. Christophersen, P.H. Nielsen, Hydrogen bonding in 3-azetidinol. I. Crystal and molecular structure, Acta Cryst. B45 (1989) 562–566.
[18] K. Hagen, H.V. Volden, U. Anthoni, C. Christophersen, M. Gajhede, P.H. Nielsen, Molecular structure and conformation of gaseous 3-azetidinol as determined by electron diffraction and ab initio calculations, J. Phys. Chem. 95 (1991) 1597–1600.
[19] U. Anthoni, D.H. Christensen, C. Christophersen, M. Gajhede, L. Henriksen, O.F. Nielsen, P.H. Nielsen, Hydrogen bonding in 3-azetidinol: Part 2. On the presence of inter- and intra-molecular interactions in solution and in the gas phase, J. Mol. Struct. 220 (1990) 43–54.
[20] T.A. Koopmans, Ordering of wave functions and eigen energies of the individual electrons of an atom, Physica 1 (1933) 104–113.
[21] K. Mandal, T. Kar, P.K. Nandi, S.P. Bhattacharyya, "Theoretical study of the nonlinear polarizabilities in H2N and NO2 substituted chromophores containing two hetero aromatic rings, Chem. Phys. Lett. 376 (1–2) (2003) 116–124.
[22] P.K. Nandi, K. Mandal, T. Kar, Effect of structural changes in sesquifulvalene on the intramolecular charge transfer and nonlinear polarizations—a theoretical study, Chem. Phys. Lett. 381 (1–2) (2003) 230–238.
[23] G. Ramesh, P. Venkata Ramana Rao, K. Srishailam, B. Venkatram Reddy, Pyridinecarboxaldehydes: Structures, Vibrational Assignments, and Molecular Characteristics Using Experimental and Theoretical Methods, Braz. J. Phy. 53 (2023) 45.
[24] K. Srishailam, L. Ravindranath, B. Venkatram Reddy, G. Ramana Rao, Electronic Spectra (Experimental and Simulated), and DFT Investigation of NLO, FMO, NBO, and MESP Characteristics of Some Biphenylcarboxaldehydes, Polycyclic Aromatic Compd. 10 (2022) 1–14.
[25] L. Ravindranath, K. Srishailam, B. Venkatram Reddy, Experimental and DFT Quantum Chemical Studies on Structural, Vibrational and Molecular Properties of Some Substituted 4-Phenylphenols, Polycyclic Aromatic Compd. (2022), https://doi.org/10.1080/10406638.2022.2161584.
[26] M.J. Frisch et al., Gaussian 09, Revision B.01, Gaussian, Inc., Wallingford CT, 2010.
[27] A.D. Becke, Density-functional thermochemistry. III. The role of exact exchange. J. Chem. Phy., 98 (1993) 5648–5652. http://doi.org/10.1063/1.464913.
[28] C. Lee, W. Yang, R.G. Parr, Development of the Colle-Salvetti correlation-energy formula into a functional of the electron density, Phys. Rev., B 37 (1988) 785–789. http://doi.org/10.1103/physrevb.37.785.
[29] D. Jacquemin, E.A. Perpète, I. Ciofini, C. Adamo, Accurate Simulation of Optical Properties in Dyes, Acc. Chem. Res. 42 (2009) 326–334, https://doi.org/10.1021/ar800163d.
[30] D. Jacquemin, J. Preat, V. Wathelet, M. Fontaine, E.A. Perpète, Thioindigo Dyes: Highly Accurate Visible Spectra with TD-DFT, J. Am. Chem. Soc. 128 (2006) 2072–2083, https://doi.org/10.1021/ja056676h.
[31] I. Ciofini, C. Adamo, Accurate Evaluation of Valence and Low-Lying Rydberg States with Standard Time-Dependent Density Functional Theory, J. Phys. Chem. A 111 (2007) 5549–5556, https://doi.org/10.1021/jp0722152.
[32] H. Gökce, Y. Sert, G. Alpaslan, A.S. El-Azab, M.M. Alanazi, M.H.M. Al-Agamy, A. A.M. Abdel-Aziz, Hirshfeld Surface, Molecular Docking Study, Spectroscopic Characterization and NLO Profile of 2-Methoxy-4,6-Diphenylnicotinonitrile, Chem. Sel. 4 (2019) 9857–9870, https://doi.org/10.1002/slct.201902391.
[33] G. Gece, The use of quantum chemical methods in corrosion inhibitor studies, Corros. Sci. 50 (2008) 2981–2992, https://doi.org/10.1016/j.corsci.2008.08.043.
[34] K. Fukui, Role of Frontier Orbitals in Chemical Reactions, Science 218 (1982) 747–754, https://doi.org/10.1126/science.218.4574.747.
[35] R.G. Parr, L.V. Szentpály, S. Liu, Electrophilicity Index, J. A Chem.. Soc. 121 (1999) 1922–1924, https://doi.org/10.1021/ja983494x.
[36] A.D. Buckingham, Permanent and Induced Molecular Moments and Long-Range Intermolecular Forces, Adv. Chem. Phys., (1967) 107–142. http://doi.org/10.1080/00268979600100491.
[37] N. Dege, H. Gökce, O.E. Doğan, G. Alpaslan, T. Ağar, S. Muthu, Y. Sert, Quantum computational, spectroscopic investigations on N-(2-((2-chloro-4,5-dicyanophenyl)amino)ethyl)-4-methylbenzenesulfonamideby DFT/TD-DFT with different solvents, molecular docking and drug-likeness researches, Colloids Surf. A: Physicochem. Eng. Asp. 638 (2022) 128311, https://doi.org/10.1016/j.colsurfa.2022.128311.
[38] E.D. Glendening, A.E. Reed, J.E. Carpenter, F. Weinhold, NBO Version 3.1 (University of Wisconsin, Madison: TCI) 1998.
[39] K.R. Acharya, S.S. Tavale, T.N.G. Row, Venkatesan K. Structure of l-Diphenylmethyl-3-hydroxyazetidinium Chloride,*$C_{16}H_{18}NO^{+}.Cl^{-}$. Acta Cryst., C40 (1984) 846–848. http://doi.org/0108-2701/84/050846-03501.50.
[40] I. Fleming, Frontier Orbitals and Organic Chemical Reactions (London :Wiley) 1976.
[41] G. Scalmani, M.J. Frisch, Continuous surface charge polarizable continuum models of solvation. I. General formalism, J. Chem. Phys. 132 (2010) 114110, https://doi.org/10.1063/1.3359469.
[42] M.D. Diener, J.M. Alford, Isolation and properties of small-bandgap fullerenes, Nature 393 (1998) 668–671, https://doi.org/10.1038/31435.
[43] R.G. Pearson, Absolute electronegativity and hardness correlated with molecular orbital theory, Proc. Natl. Acad. Sci. USA 83 (1986) 8440–8441, https://doi.org/10.1073/pnas.83.22.8440.
[44] Z. Demircioğlu, C.A. Kaştaş, O. Büyükgüngör, The spectroscopic (FT-IR, UV–vis), Fukui function, NLO, NBO, NPA and tautomerism effect analysis of (E)-2-[(2-hydroxy-6-methoxybenzylidene)amino]benzonitrile, Spectrochim. Acta Part A 139 (2015) 539–548, https://doi.org/10.1016/j.saa.2014.11.078.
[45] Y.X. Sun, Q.L. Hao, W.X. Wei, Z.X. Yu, L.D. Lu, X. Wang, Y.S. Wang, Experimental and density functional studies on 4-(4-cyanobenzylideneamino)antipyrine, Mol. Phys. 107 (2009) 223–235, https://doi.org/10.1080/00268970902769471.
[46] C. Andraud, T. Brotin, C. Garcia, F. Pell, P. Goldner, B. Bigot, A. Collet, Theoretical and experimental investigations of the nonlinear optical properties of vanillin, polyenovanillin, and bisvanillin derivatives, J. Am. Chem. Soc. 116 (1994) 2094–2102.
[47] K.S. Pitzer, The Vibration Frequencies and Thermodynamic Functions of Long Chain Hydrocarbons, Mol Struc Stat Therm. (1993:) 22–31, https://doi.org/10.1142/9789812795960_0006.
[48] M.M. Ghahremanpour, P.J.V. Maaren, J.C. Ditz, R. Lindh, D.V. Spoel, Large-scale calculations of gas phase thermochemistry: Enthalpy of formation, standard entropy, and heat capacity, J. Chem. Phys. 145 (2016), https://doi.org/10.1063/1.4962627.

[49] E. Scrocco, J. Tomasi, Electronic Molecular Structure, Reactivity and Intermolecular Forces: An Euristic Interpretation by Means of Electrostatic Molecular Potentials, Adv. Quant. Chem. 11 (1979) 115–193, https://doi.org/10.1016/S0065-3276(08)60236-1.

[50] F.J. Luque, J.M. López, M. Orozco, Perspective on "Electrostatic interactions of a solute with a continuum. A direct utilization of ab initio molecular potentials for the prevision of solvent effects, Theoret. Chem. Acc., 103 (2000) 343–345. http://doi.org/10.1007/s002149900013.

[51] N. Okulik, A.H. Jubert, Theoretical Analysis of the Reactive Sites of Non–steroidal Anti–inflammatory Drugs, Internet Electron. J. Mol. Des. (BioChem Press) 4 (2005) 17–30.

[52] N. Mohan, C.H. Suresh, A. Kumar, S.R. Gadre, Molecular electrostatics for probing lone pair–π interactions, Phy. Chem. Chem. Phys. 15 (2013) 18401–18409, https://doi.org/10.1039/C3CP53379D.

[53] C.H. Suresh, S.R. Gadre, Clar's Aromatic Sextet Theory Revisited via Molecular Electrostatic Potential Topography, J. Organic Chem. 64 (1999) 2505–2512, https://doi.org/10.1021/jo990050q.

[54] P.K. Anjalikrishna, C.H. Suresh, S.R. Gadre, Electrostatic Topographical Viewpoint of π-Conjugation and Aromaticity of Hydrocarbons, J. Phys. Chem. 123 (2019) 10139–10151, https://doi.org/10.1021/acs.jpca.9b09056.